ISSN 1063-7745, Crystallography Reports, 2024, Vol. 69, No. 4, pp. 478–484. © Pleiades Publishing, Inc., 2024.

## STRUCTURE OF INORGANIC COMPOUNDS

# Novel Ternary Intermetallic Compounds $R_4Ru_2Ga_3$ ($R$ = Pr, Nd, Sm, Gd, Tb, Dy, Ho, Er)

**I. A. Grekhov**[a], **Zh. M. Kurenbaeva**[a], **and E. V. Murashova**[a],*

[a] *Department of Chemistry, Lomonosov Moscow State University, Moscow, 119991 Russia*

**e-mail: lena1960murashova@gmail.com*

Received September 11, 2023; revised October 16, 2023; accepted October 16, 2023

**Abstract**—A number of new isostructural ternary intermetallic compounds of the composition $R_4Ru_2Ga_3$ ($R$ = Pr, Nd, Sm, Gd, Tb, Dy, Ho, Er) were found in ternary $R$–Ru–Ga systems. The single-crystal X-ray diffraction study of $Nd_4Ru_2Ga_3$ showed that this compound crystallizes in the monoclinic system and it is a representative of a new structure type ($a$ = 10.938(6) Å, $b$ = 4.064(2) Å, $c$ = 9.746(5) Å, $\beta$ = 111.18(2)°, space group $C2$, $Z$ = 2, $R1$ = 0.043, $wR2$ = 0.060 for 1198 reflections). The specific structural feature of this compound is the presence of distorted $RuNd_6$ ($AlB_2$ type) and $GaNd_8$ (CsCl type) units. The shortest Nd–Ru distance in the polyhedron is 2.8463(16) Å, which is significantly smaller than the sum of the corresponding atomic radii. The unit cell parameters and volumes in the $R_4Ru_2Ga_3$ series ($R$ = Pr, Nd, Sm, Gd, Tb, Dy, Ho, Er) decrease in accordance with lanthanide compression, while their melting points increase.

**DOI:** 10.1134/S1063774523601570

## INTRODUCTION

Ternary ruthenium gallides with a high content of rare-earth elements ($R$) are known primarily for lanthanum and cerium. Examples are $Ce_9Ru_4Ga_5$ [1], $Ce_6Ru_{0.48}Ga_{2.52}$, $Ce_{23}Ru_7Ga_4$ [2], $Ce_4Ru_3Ga_3$, $La_3Ru_2Ga_2$ [3], $R_5Ru_3Ga_2$ ($R$ = La–Nd) [4], and $R_{26}(Ru_{1-x}Ga_x)_{17}$ ($R$ = Ce, Y, Tb, Dy, Ho, Er, Tm, Lu) [5]. When searching for analogs of the intermetallic compound $La_3Ru_2Ga_2$ containing rare-earth elements $R$ = Pr, Nd, Sm, Gd, Tb, Dy, Ho, Er, we found a series of compounds of the composition $R_4Ru_2Ga_3$, which crystallize in a new structure type. The isoformula compounds $R_4Co_2Mg_3$ ($R$ = Pr, Nd, Sm, Gd, Tb, Dy) crystallize in their own structure type and are built from $AlB_2$- and CsCl-type units in a ratio of 1 : 3 [6]. The intermetallic compound $Gd_4Co_2Mg_3$ belonging to this series is characterized by the magnetic ordering at $T_N$ = 75(1) K and exhibits the magnetocaloric effect [7]. Among gallides with the same stoichiometry, there is the ternary compound $Ti_4Ni_2Ga_3$ with the structure derived from ZrNiAl [8]. Here, we report the results of the synthesis and the structural and thermal characteristics of the synthesized compounds. The crystal-chemical comparison of the structures of the new compounds with the structures of the known isoformula compounds and other intermetallics with a similar composition was performed.

## EXPERIMENTAL

The samples were prepared from stoichiometric amounts of the elemental components $R$ (44.45 at %), Ru (22.22 at %), and Ga (33.33 at %) by the high-temperature liquid-phases synthesis in an electric arc using a laboratory mini arc melter MAM-1 (Bühler) equipped with a non-consumable tungsten electrode on a water-cooled copper plate under an argon atmosphere. Zirconium was used as the getter. The starting metals have the following degree of purity: $R$, 99.8 wt %; Ru, 99.97 wt %; Ga, 99.999 wt %. The samples were remelted several times by turning them upside down after each solidification to ensure complete fusion and homogeneity. The alloys were brought to an equilibrium state by performing the annealing in evacuated quartz tubes, which were placed in muffle furnaces at 600°C for 1000 h, followed by the quenching in ice water.

The samples obtained by the annealing were studied by electron-probe X-ray microanalysis on a LEO EVO 50XPV scanning electron microscope equipped with an OXFORD INSTRUMENTS INCA-energy 450 energy-dispersive analysis system operating at an accelerating voltage of 20 kV and by X-ray powder diffraction analysis on an automated STOE STADI P X-ray powder diffractometer ($CuK_{\alpha1}$ radiation, Ge monochromator, linear detector, WinXPOW software [9]).

The structure was determined using single crystals of $Nd_4Ru_2Ga_3$, which were selected from a crushed annealed sample. The experimental data were col-

**Table 1.** Crystallographic parameters and the X ray diffraction data collection and structure refinement statistics for a single crystal of $Nd_4Ru_2Ga_3$

| Molecular formula | $Nd_4Ru_2Ga_3$ |
|---|---|
| Molecular weight | 988.26 |
| Composition, at % | 44.1 Nd 22.6 Ru 33.3Ga |
| Crystal system, sp. gr., $Z$ | Monoclinic, $C2$, 2 |
| $a$, $b$, $c$, Å | 10.899(3), 4.0533(11), 9.720(3) |
| β, deg | 111.080(7) |
| $V$, Å$^3$ | 400.7(2) |
| $D_{calc}$, g/cm$^3$ | 8.192 |
| Temperature, K | 250(2) |
| Radiation; λ, Å | Mo$K_\alpha$; 0.71073 |
| μ, mm$^{-1}$ | 19.438 |
| $F(000)$ | 421 |
| Crystal size, mm | 0.08 × 0.04 × 0.02 |
| $\theta_{min}$–$\theta_{max}$, deg | 2.246–33.275 |
| $hkl$ ranges | $-16 \le h \le 16$, $-6 \le k \le 6$, $-14 \le l \le 14$ |
| Number of reflections: measured ($N1$)/unique with $I \ge 2\sigma(I)$ ($N2$), $R_{int}$ | 3219/1518, 0.0393 |
| Completeness of data to θ = 25.242° | 100.0% |
| Absorption correction | Semiempirical |
| $T_{min}$, $T_{max}$ | 0.1044, 0.0495 |
| Refinement method | Full-matrix least squares based on $F^2$ |
| Number of refined parameters | 47 |
| $R1/wR2$ based on $N1$ | 0.0600/0.0811 |
| $R1/wR2$ based on $N2$ | 0.0429/0.0765 |
| $S$ | 1.142 |
| Flack parameter | 0.4(2) |
| $\Delta\rho_{min}/\Delta\rho_{max}$, e/Å$^3$ | −1.176/1.360 |

**Table 2.** Atomic coordinates and atomic displacement parameters $U_{eq}$ in the structure of $Nd_4Ru_2Ga_3$

| Atom | $x/a$ | $y/b$ | $z/c$ | $U_{eq}$, Å$^2$ |
|---|---|---|---|---|
| Nd(1) | 0.2456(1) | −0.0054(6) | 0.1465(1) | 0.013(1) |
| Nd(2) | −0.0983(1) | 0.4969(7) | −0.3657(1) | 0.013(1) |
| Ru(1) | 0.0436(1) | −0.0050(17) | −0.1376(1) | 0.024(1) |
| Ga(1) | 0.1078(2) | −0.0058(15) | −0.3805(2) | 0.017(1) |
| Ga(2)* | −0.0074(12) | 0.4840(30) | 0.0172(10) | 0.014(1) |

* The site occupancy for the Ga(2) atom is 50%.

lected on an automated Bruker APEX3 X-ray diffractometer (Mo$K_\alpha$ radiation) by standard procedures at room temperature. Principal crystallographic data and the structure refinement statistics are summarized in Table 1. The structure solution and refinement were performed using the SHELXL2018 program package [10, 11]. The atomic coordinates in the $Nd_4Ru_2Ga_3$ structure are given in Table 2. Selected interatomic distances are listed in Table 3. The structural data were deposited via the joint CCDC/FIZ Karlsruhe deposition service (deposition number 2294066 for $Nd_4Ru_2Ga_3$).

The structures of intermetallics with other rare-earth elements were refined by the Rietveld method based on the X-ray powder diffraction patterns of the samples using the FULLPROF software [12, 13] and $Nd_4Ru_2Ga_3$ as the structural model (Table 4).

The melting points of the synthesized compounds were determined using a NETZSCH Leading Thermal Analysis STA 449 F1 Jupiter Platinum RT differential scanning calorimeter in a high-purity helium atmosphere in the temperature range of 30–1500°C. The heating rate was 20 deg/min. The weight of the sample was not higher than 0.05 g.

## RESULTS AND DISCUSSION

All the obtained samples contained the intermetallic compound of the composition $R_4Ru_2Ga_3$, isostructural with $Nd_4Ru_2Ga_3$, as the main phase. No more than two impurity phases were present in each sample. The following impurity phases were found in the samples: binary gallides $R$Ga (TlI type [14]) and also phases of variable composition, such as $RRu_{1-x}Ga_x$ (CsCl type [15]), $RRu_{2-x}Ga_x$ with a structure derived from the low-temperature hexagonal modification of $RRu_2$ [16] ($MgZn_2$ type) or its high-temperature cubic modification ($MgCu_2$ type) [17], and $R_{26}(Ru_{1-x}Ga_x)_{17}$ [5]. The ternary intermetallic compound $Pr_5Ru_3Ga_2$ [4] was present as one of impurity phases in the praseodymium-containing sample. The neodymium- and erbium-containing samples were the purest in terms of phase; the total content of impurities in these samples was not higher than 5 and 6 wt %, respectively (Fig. 1). The microstructure of these samples (Fig. 2) contains the same phases as those found in the X-ray powder diffraction patterns of $Nd_4Ru_2Ga_3$ and $Er_4Ru_2Ga_3$.

The Rietveld refinement was performed using the structural model of the $Nd_4Ru_2Ga_3$ single crystal, which was found in the crushed sample. The X-ray diffraction analysis demonstrated that the crystal structure of $Nd_4Ru_2Ga_3$ belongs to the monoclinic system and it is a representative of a new structure type (Table 1). The possible space groups were $C2/m$, $C2$, and $Cm$. The structure refinement of $Nd_4Ru_2Ga_3$ in the centrosymmetric space group led to highly elon-

**Table 3.** Selected interatomic distances in the structure of $Nd_4Ru_2Ga_3$

| Distance | *d*, Å | Distance | *d*, Å | Distance | *d*, Å | Distance | *d*, Å |
|---|---|---|---|---|---|---|---|
| Nd(1)–Ru(1) | 2.8463(16) | Nd(2)–Ru(1) | 2.986(5) | –Nd(1) | 2.8463(16) | | 3.154(2) |
| | 3.088(5) | | 2.996(5) | –Nd(2) | 2.986(5) | | 3.159(5) |
| | 3.090(5) | –Ga(1) | 3.060(5) | | 2.996(5) | | 3.173(4) |
| | 3.1211(18) | | 3.074(5) | –Nd(1) | 3.088(5) | CN of Ga(1) | 9 |
| –Ga(1) | 3.035(4) | | 3.154(2) | | 3.090(5) | Ga(2)–Ru(1) | 2.405(11) × 2 |
| | 3.037(5) | | 3.159(5) | | 3.1211(18) | | 2.665(9) |
| –Ga(2) | 3.200(12) | –Ga(2) | 3.161(9) | CN of Ru(1) | 9 | | 2.479(11) × 2 |
| | 3.260(12) | | 3.490(9) | | | | 2.732(10) |
| | 3.253(12) | –Ga(1) | 3.173(4) | Ga(1)–Ga(1) | | –Nd(1) | 3.200(12) × 2 |
| | 3.312(12) | | 3.6642(13) | –Ru(1) | | | 3.260(12) |
| | 3.356(7) | –Nd(1) | 3.693(2) | | | | 3.253(12) × 2 |
| | 3.734(14) | | 3.704(2) | –Nd(1) | | | 3.312(12) |
| –Nd(1) | 3.5254(15) × 2 | CN of Nd(2) | 11 | | 2.644(4) | | 3.356(7) × 2 |
| –Nd(2) | 3.6642(13) | Ru(1)–Ga(2) | 2.405(11) | | 2.693(2) | | 3.734(14) |
| | 3.693(2) | | 2.665(9) | | 3.035(4) | –Nd(2) | 3.161(9) × 2 |
| | 3.704(2) | | 2.479(11) | | 3.037(5) | | 3.490(9) |
| CN of Nd(1) | 14 | | 2.732(10) | –Nd(2) | 3.060(5) | CN of Gd(2) | 12 |
| | | –Ga(1) | 2.693(2) | | 3.074(5) | | |

**Table 4.** Monoclinic unit cell parameters and volumes and the melting points of the compounds $R_4Ru_2Ga_3$ ($R$ = Pr, Nd, Sm, Gd, Tb, Dy, Ho, Er)

| Compound | *a*, Å | *b*, Å | *c*, Å | β, deg | *V*, $Å^3$ | $T_m$,°C |
|---|---|---|---|---|---|---|
| $Pr_4Ru_2Ga_3$ | 10.9303(4) | 4.2388(1) | 9.6634(3) | 111.014(3) | 417.95(2) | 741 |
| $Nd_4Ru_2Ga_3$ | 10.9055(4) | 4.1865(1) | 9.6757(3) | 111.070(3) | 412.21(2) | 811 |
| $Sm_4Ru_2Ga_3$ | 10.8588(4) | 4.0917(2) | 9.6920(4) | 111.077(4) | 401.82(3) | 848 |
| $Gd_4Ru_2Ga_3$ | 10.8278(3) | 4.0154(1) | 9.7234(3) | 111.150(3) | 394.27(2) | 926 |
| $Tb_4Ru_2Ga_3$ | 10.7857(5) | 3.9705(2) | 9.7073(4) | 111.264(3) | 387.41(3) | 953 |
| $Dy_4Ru_2Ga_3$ | 10.7214(7) | 3.9616(2) | 9.6912(7) | 111.298(6) | 383.51(4) | 977 |
| $Ho_4Ru_2Ga_3$ | 10.6797(3) | 3.9441(1) | 9.6834(2) | 111.352(2) | 379.88(2) | 1002 |
| $Er_4Ru_2Ga_3$ | 10.6347(2) | 3.9225(1) | 9.6644(1) | 111.411(1) | 375.32(1) | 1058 |

gated displacement ellipsoids for the Ru and Ga2 atoms. The lowering of the symmetry to *Cm* or *C*2 resulted in the normal sizes of the displacement ellipsoids, but the *R* factors in sp. gr. *C*2 were somewhat lower than those in sp. gr. *Cm*. In sp. gr. *C*2, the Ga2 atom is disordered over two positions about the twofold axis. The unit cell parameters and volumes refined by the Rietveld method for the whole series of the compounds $R_4Ru_2Ga_3$, where $R$ = Pr, Nd, Sm, Gd, Tb, Dy, Ho, Er (Table 4), decrease in the series from praseodymium to erbium in accordance with lanthanide compression.

The crystal structure of $Nd_4Ru_2Ga_3$ contains five crystallographically independent atoms in the 4*c* sites: two neodymium atoms, one ruthenium atom, and two gallium atoms. The Ga2 atom is displaced from the 2*b* site and, therefore, the occupancy of the 4*c* site is 0.5. The nearest environment of the ruthenium atom involves six neodymium atoms and three gallium atoms, which form a tricapped trigonal prism (CN = 9; CN is the coordination number) (Fig. 3). The coordination environment of the Ga1 atom can be described as a seven-vertex polyhedron formed by neodymium atoms and supplemented by two addi-

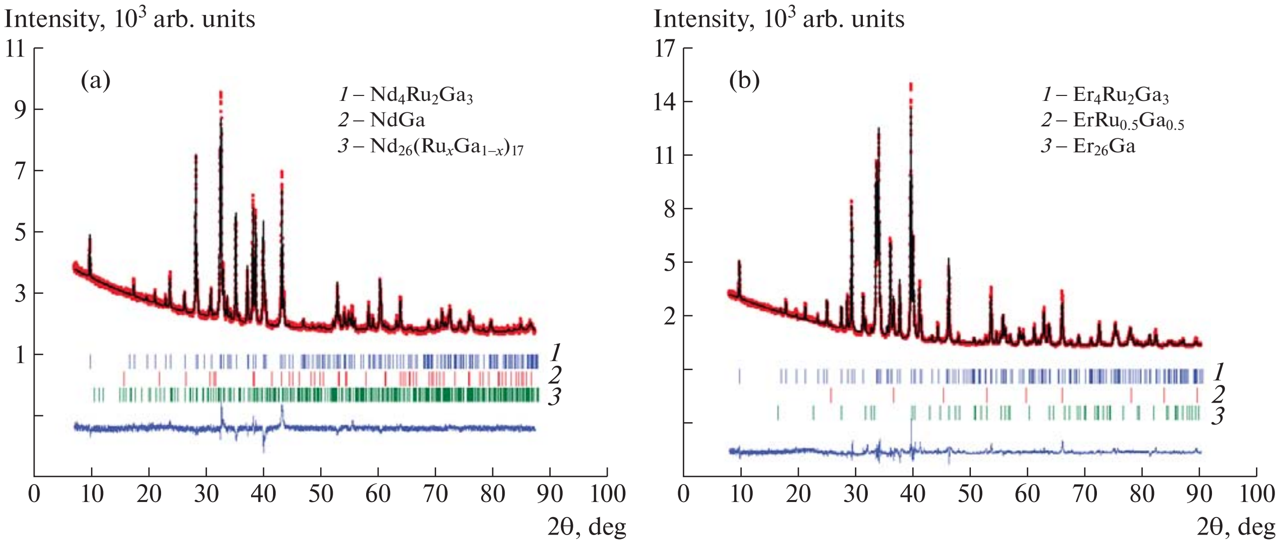

**Fig. 1.** Rietveld refinement of the structures of (a) $Nd_4Ru_2Ga_3$ and (b) $Er_4Ru_2Ga_3$ in the presence of traces of admixtures based on the powder X-ray diffraction patterns: the experimental data (small circles), the simulated patterns (solid lines), and the difference plots (at the bottom). The positions of the Bragg reflections are indicated by vertical bars.

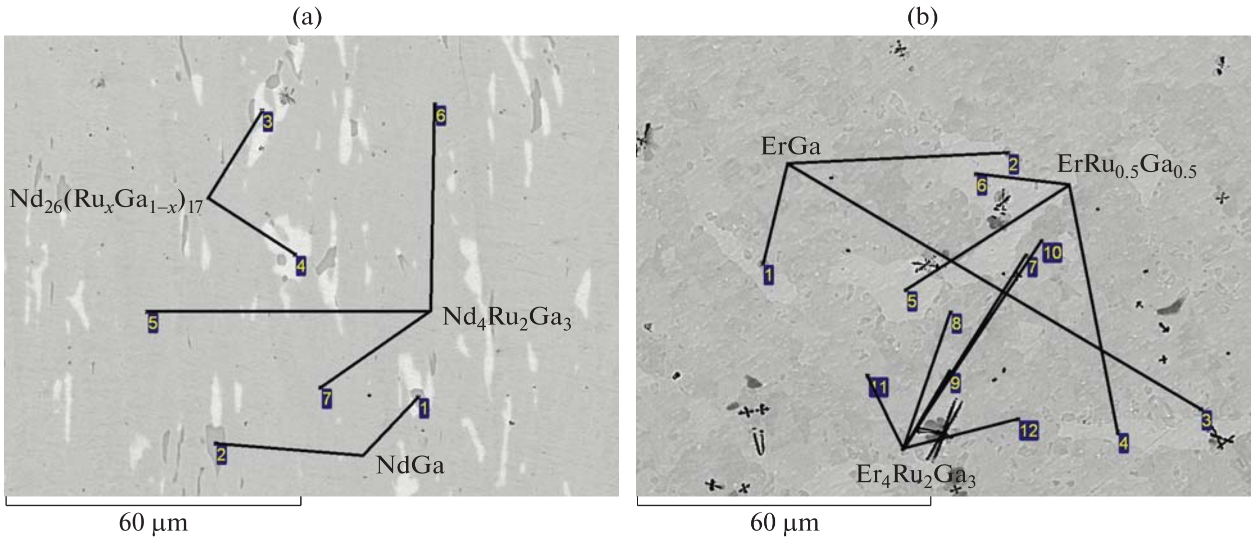

**Fig. 2.** Microstructure of annealed samples of (a) $Nd_4Ru_2Ga_3$ and (b) $Er_4Ru_2Ga_3$.

tional gallium and ruthenium atoms (CN = 9). The coordination environment of the Ga2 atom is a strongly distorted tetragonal prism formed by neodymium atoms and four ruthenium atoms above the lateral faces (CN = 12). The Nd1 atom is at the center of the pentagonal prism formed by four neodymium atoms, four gallium atoms, and two ruthenium atoms. Four of the five rectangular lateral faces are centered by two ruthenium atoms, one gallium atom, and one neodymium atom (CN = 14). The Nd2 atom is at the center of the tetragonal prism formed by four gallium atoms, two ruthenium atoms, and two neodymium atoms. The lateral faces are centered by two gallium atoms and one neodymium atom (CN = 11).

Overall, the $Nd_4Ru_2Ga_3$ structure can be represented as a layered structure, in which the corrugated layers of neodymium atoms alternate with the layers formed by ruthenium and gallium atoms along the [001] direction (Fig. 4a). The networks of ruthenium and gallium atoms contain a fragment as a chain of rhombuses (Fig. 4b) formed by ruthenium and gallium atoms. A similar fragment is present in other structures containing ruthenium and gallium, such as $La_3Ru_2Ga_2$

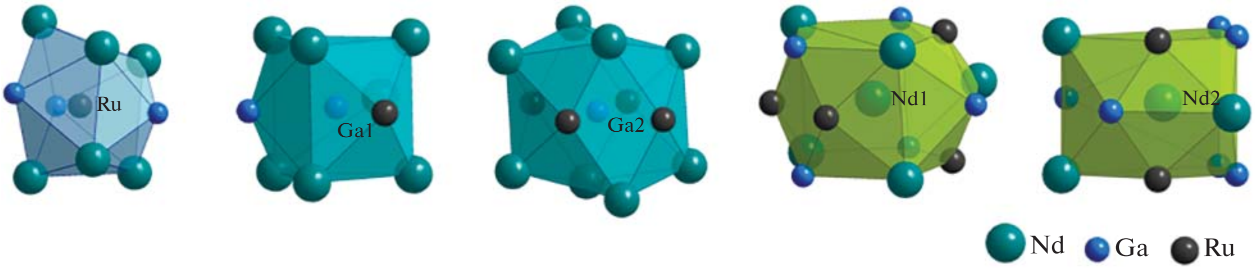

**Fig. 3.** Coordination polyhedra of atoms in the $Nd_4Ru_2Ga_3$ structure.

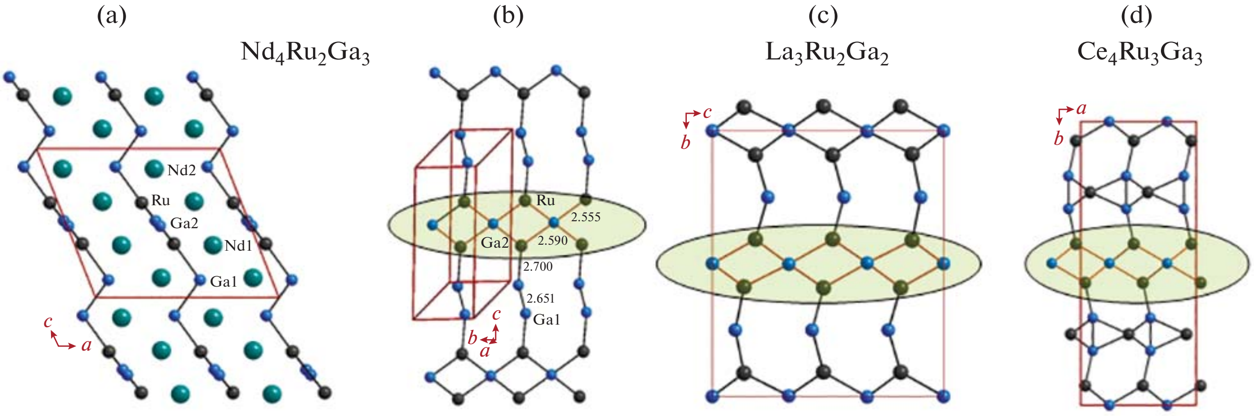

**Fig. 4.** (a) Projection of the $Nd_4Ru_2Ga_3$ structure along the [010] axis. Networks of Ru and Ga atoms in the structures of (b) $Nd_4Ru_2Ga_3$ (the disorder of Ga2 is not shown for the sake of clarity), (c) $La_3Ru_2Ga_2$, and (d) $Ce_4Ru_3Ga_3$. The chains consisting of ruthenium and gallium atoms are indicated by ovals.

(Fig. 4c) and $Ce_4Ru_3Ga_3$ (Fig. 4d). In the $Nd_4Ru_2Ga_3$ structure, all atoms that form the rhombuses in the chains lie in one plane. In the $La_3Ru_2Ga_2$ and $Ce_4Ru_3Ga_3$ structures, the rhombuses are rotated with respect to each other.

In the $Nd_4Ru_2Ga_3$ structure, the Ru–Ga distances are the shortest of all the distances (2.405(11)–2.732(10) Å). These distances are smaller than the sum of the atomic radii ($r$(Ru) = 1.34 Å, $r$(Ga) = 1.41 Å [18]), which is indicative of a significant interaction between the ruthenium and gallium atoms. The distances between the neodymium atoms in the networks are longer than 3.5254(15) Å, and the distances to the atoms of the adjacent Ru/Ga network are abnormally long. One of the Nd–Ru distances is 2.8463(16) Å, which is smaller not only than the sum of the atomic radii (3.16 Å) but also than the sum of the covalent radii (2.88 Å). This may be an evidence of a significant chemical bonding of these atoms. The other Nd–Ru distances in the Ru polyhedron are only slightly smaller than the sum of the atomic radii.

The $Nd_4Ru_2Ga_3$ structure can also be represented as a combination of fragments of the known $AlB_2$ and CsCl structure types. The $RuNd_6$ trigonal prism is a fragment of the $AlB_2$-type structure. The adjacent $RuNd_6$ trigonal prisms are linked together by sharing edges to form a group of four trigonal prisms (Fig. 5a). The interatomic Ru–Ru distances in the adjacent prisms are 3.143(3) Å, which are larger than the sum of the atomic radii. Like in the CsCl structure type, the gallium atom Ga2 is at the center of a distorted tetragonal prism. Similar fragments are observed in some indides ($R_{11}Ru_4In_9$ R = Ce, Gd, Tb) [19, 20] (Fig. 5b).

The structure of the isoformula compound $R_4Co_2Mg_3$ (Fig. 5c) is also built from $AlB_2$ and CsCl units in a ratio of 1 : 3 [6]. The common feature of the structures of indides $R_{11}Ru_4In_9$ and the magnesium-containing compounds $R_4Co_2Mg_3$ is the orientation of the $AlB_2$-type trigonal prisms and distorted CsCl-type tetragonal prisms along the smallest unit cell parameter so that this parameter is the height of both the trigonal and tetragonal prisms. In the $R_4Co_2Mg_3$ structure, the $CoR_6$ trigonal prisms are linked in pairs via a shared quadrangular face. It should be mentioned that the Co–Co distances in the pair are abnormally short (2.37 Å). All magnesium atoms are at the centers of CsCl-type tetragonal prisms.

In the $Nd_4Ru_2Ga_3$ structure, only the Ga2 atom is in a distorted CsCl-type eight-vertex polyhedron, the distances to the neodymium atoms in the polyhedron

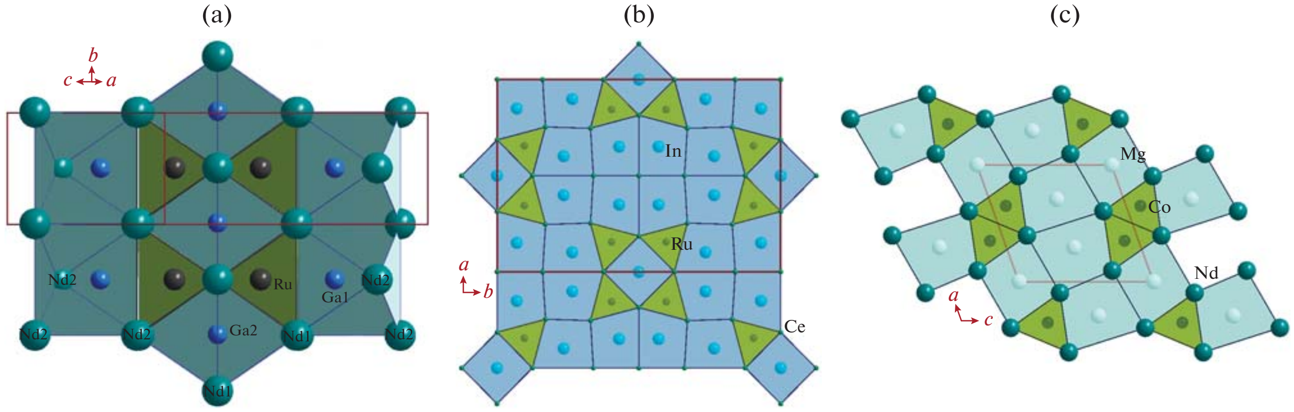

**Fig. 5.** (a) Fragment of the $Nd_4Ru_2Ga_3$ structure consisting of $AlB_2$-type trigonal prisms $RuNd_6$ and CsCl-type tetragonal prisms $GaNd_8$. Projections of the (b) $Ce_{11}Ru_4In_9$ and (c) $Nd_4Co_2Mg_3$ structures consisting of $AlB_2$- and CsCl-type polyhedra along the smallest unit cell parameter.

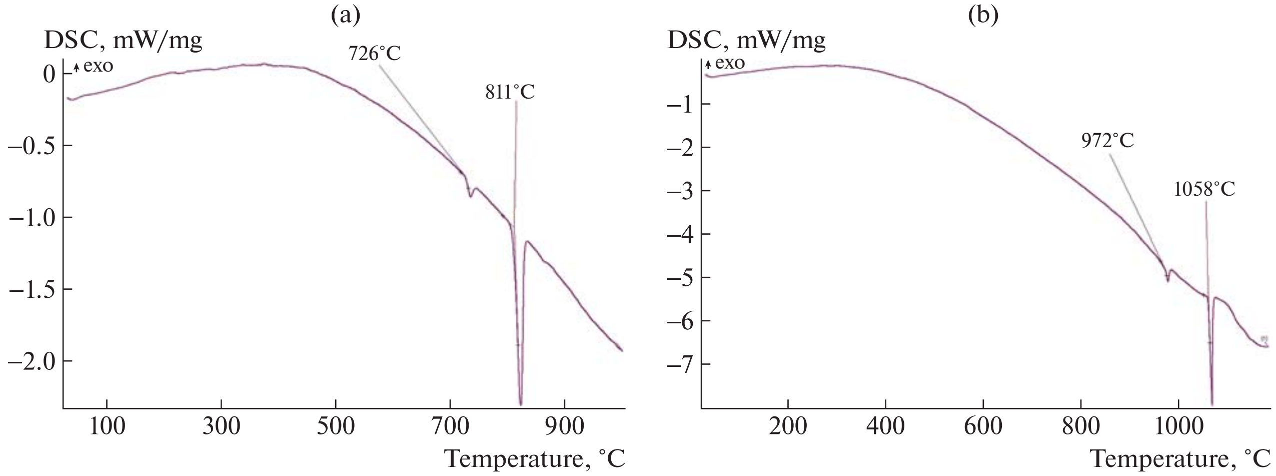

**Fig. 6.** Thermograms of (a) $Nd_4Ru_2Ga_3$ and (b) $Er_4Ru_2Ga_3$.

being longer than 3.161(9) Å, which is larger than the sum of their atomic radii. Probably, it is this fact that is responsible for the disorder of the Ga2 atom, because the void formed by neodymium atoms is too large. The environment of the Ga1 atom is a seven-vertex polyhedron formed by neodymium atoms. The distances in this polyhedron are smaller than or equal to the sum of the atomic radii of neodymium and gallium atoms. This polyhedron can be described as a distorted cube with one degenerate vertex. Overall, the structure can be represented as a combination of $AlB_2$-type and CsCl-type units, and only a part of CsCl units can be considered as degenerate polyhedra. As opposed to the structures containing magnesium and indium, the layers in the $Nd_4Ru_2Ga_3$ structure are non-planar and are perpendicular to the *a* axis (Fig. 4a). The smallest parameter *b* in the $Nd_4Ru_2Ga_3$ structure is equal to the edge length of one of the triangular bases rather than to the height of the $RuNd_6$ trigonal prism.

The investigation of the thermal stability of the obtained compounds $R_4Ru_2Ga_3$ was complicated by the presence of impurities in the samples. The thermograms show weak peaks attributed to the presence of these impurities (Fig. 6). The strongest endothermic peaks were assigned to the melting of the main phase. The melting led to a change in the initial shape of the sample. The melting points of the whole series of the compounds $R_4Ru_2Ga_3$ were determined (Table 4). Their values increase in the series from $Pr_4Ru_2Ga_3$ to $Er_4Ru_2Ga_3$. The X-ray diffraction patterns of the samples after the melting were not completely identical to the X-ray diffraction pattern of the sample before the melting. The X-ray diffraction pattern of $Nd_4Ru_2Ga_3$ has, apart from reflections belonging to the main phase, reflections assigned to $NdRu_{2-x}Ga_x$ with the $MgZn_2$ structure. After the melting of the compounds $R_4Ru_2Ga_3$ with $R$ = Ho, Er, the compounds $RRu_{2-x}Ga_x$

with the $MgZn_2$ structure and $RRu_{1-x}Ga_x$ with the CsCl structure were obtained.

## CONCLUSION

In the ternary $R$–Ru–Ga systems, a series of isostructural compounds $R_4Ru_2Ga_3$ ($R$ = Pr, Nd, Sm, Gd, Tb, Dy, Ho, Er) belonging to a new structure type were obtained. The unit cell parameters and volumes in the series of these compound decrease in accordance with lanthanide compression. The compounds are stable in air and do not decompose during the investigation and storage. In the crystal structure, $AlB_2$- and CsCl,-type units can be observed; however, they are highly distorted. The fragment of the $R_4Ru_2Ga_3$ structure as a chain of rhombuses, which are formed by ruthenium and gallium atoms, was found also in the $La_3Ru_2Ga_2$ and $Ce_4Ru_3Ga_3$ structures. Based on the analysis of the interatomic distances in the $Nd_4Ru_2Ga_3$ structure, it can be stated that there is a significant chemical bonding between the ruthenium and gallium atoms and between the neodymium and ruthenium atoms. The melting points of the obtained compounds increase in the series from $Pr_4Ru_2Ga_3$ to $Er_4Ru_2Ga_3$.

## FUNDING

This study was performed within the framework of the state assignment (No. AAAA-A21-121011590083-9) under the theme “Fundamentals of the design of metallic and composite materials.” The experimental data for the X-ray diffraction analysis were obtained using the equipment of the Joint Research Center of the N. S. Kurnakov Institute of General and Inorganic Chemistry of the Russian Academy of Sciences (JRC IGIC RAS).

## CONFLICT OF INTEREST

The authors declare that they have no conflicts of interest.

## REFERENCES

1. K. Shablinskaya, E. Murashova, A. Tursina, et al., Intermetallics **23**, 106 (2012). https://doi.org/10.1016/j.intermet.2011.12.024
2. E. V. Murashova and Zh. Kurenbaeva, Inorg. Mater. **55** (8), 785 (2019).
3. K. Shablinskaya, E. Murashova, Zh. Kurenbaeva, et al., J. Alloys Compd. **575**, 183 (2013). https://doi.org/10.1016/j.jallcom.2013.04.021
4. E. Murashova, A. Tursina, Zh. Kurenbaeva, et al., J. Alloys Compd. **871**, 159538 (2021). https://doi.org/10.1016/j.jallcom.2021.159538
5. O. R. Myakush, A. A. Fedorchuk, and A. V. Zelinskii, Inorg. Mater. **34** (6), 562 (1998).
6. M. Kersting, U. Ch. Rodewald, and R. Pöttgen, Z. Kristallogr. **230** (3), 151 (2015). https://doi.org/10.1515/zkri-2014-1831
7. S. Gorsse, B. Chevalier, S. Tuncel, and R. Pöttgen, J. Solid State Chem. **182**, 948 (2009). https://doi.org/10.1016/j.jssc.2009.01.027
8. V. Ja. Markiv, N. N. Beljavina, A. A. L’isenko, and A. A. Babenko, Dopov. Akad. Nauk Ukr. RSR. B **1**, 35 (1983).
9. *STOE WINXPOW, Version 2. 24* (Stoe & Cie GmbH, Darmstadt, Germany, 2009).
10. G. M. Sheldrick, Acta Crystallogr. C **71**, 3 (2015). https://doi.org/10.1107/S2053229614024218
11. G. M. Sheldrick, *SADABS.* (Univ. of Göttingen, Göttingen, 2004).
12. J. Rodriguez-Carvajal, Physica B **192**, 55 (1993). https://doi.org/10.1016/ 0921-4526(93)90108-I
13. T. Roisnel and J. Rodriguez-Carvajal, Mater. Sci. Forum. **378–381**, 118 (2000). https://doi.org/. scientific.net/MSF.378-381.118 https://doi.org/10.4028/www
14. S. P. Yatsenko, A. A. Semyannikov, B. G. Semenov, and K. A. Chuntonov, J. Less-Comm. Met. **64**, 185 (1979).
15. D. Sedel’nikov, Yu. Grishina, A. Tursina, et al., Inorg. Mater. **58** (6), 568 (2022).
16. A. E. Dwight, J. W. Downey, and R. A. Conner, Jr., Trans. Metall. Soc. AIME **236**, 1509 (1966).
17. J. F. Cannon, D. L. Robertson, and H. T. Hall, J. Less-Comm. Met. **29**, 141 (1972).
18. J. Emsley, *The Elements* (Oxford Univ. Press, Oxford, 1999), p. 255.
19. V. Gribanova, E. Murashova, D. Gnida, et al., J. Alloys Compd. **711**, 455 (2017). https://doi.org/10.1016/j.jallcom.2017.03.168
20. A. Tursina, V. Chernyshev, S. Nesterenko, et al., J. Alloys Compd. **791**, 641 (2019). https://doi.org/10.1016/j.jallcom.2019.03.224

*Translated by T. Safonova*

SPELL: OK